Journal of Volcanology and Geothermal Research 432 (2022) 107707

Contents lists available at ScienceDirect

Journal of Volcanology and Geothermal Research

journal homepage: www.journals.elsevier.com/journal-of-volcanology-and-geothermal-research

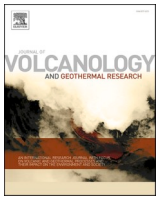

Long range infrasound monitoring of Yasur volcano

Rebecca Sveva Morelli [a,b,*], Duccio Gheri [a], Paola Campus [c], Diego Coppola [d], Emanuele Marchetti [a]

[a] Department of Earth Sciences, University of Firenze, via G. La Pira 4, 50121 Firenze, Italy
[b] National Institute of Geophysics and Volcanology, Osservatorio Vesuviano, via Diocleziano 328, 80124 Napoli, Italy
[c] CTBTO, Vienna, Austria
[d] Department of Earth Sciences, University of Torino, via Valperga Caluso 35, 10125 Torino, Italy

ARTICLE INFO

Keywords:
Infrasound
Volcano
International monitoring system
Satellite
Yasur

ABSTRACT

The atmospheric injection of gas and material produced by an explosive volcanic eruption determines a rapid compression of the atmosphere, which subsequently propagates as longitudinal elastic waves (sound). The size of the source, generally greater than tens of meters, and its duration, longer than a few seconds, result into an emitted signal that is particularly rich in low frequencies ($f < 20$ Hz), thus determining an efficient infrasound radiation. Thanks to the low spectral content and the reduced attenuation in the atmosphere, infrasound is capable of propagating for very large distances.

In this study we show how the infrasonic monitoring at regional distances (> 100 km) is efficient in recording and characterizing volcanic events. For the purpose of our study, infrasound signal radiated from Yasur volcano (Tanna Island, Vanuatu) was studied for a period of twelve years (January 2008 – December 2019). Signals from Yasur were registered at a source-to-receiver distance of 400 km by the IS22 infrasound array, located in New Caledonia, part of the Comprehensive Nuclear-Test-Ban Treaty (CTBT) International Monitoring System (IMS). The predominantly explosive Strombolian activity of this volcano makes it a perfect subject to be studied by infrasound technology. Detections of volcanic infrasound are modulated according to the seasonal variation of stratospheric winds and corrected for attenuation accounting for real atmospheric specification between the source and the receiver to retrieve the pressure at the source. Next, they are used to evaluate long-term (yearly) and short term (hourly) variations of activity over the period of analysis. Results are compared with thermal anomalies recorded by the MODerate resolution Imaging Spectroradiometer (MODIS) installed on NASA's Terra and Aqua satellites.

We show that even at regional distances (400 km) it is possible to follow the long term (yearly) fluctuations of ordinary explosive activity during periods of optimal propagation of infrasonic waves in the atmosphere. In addition, we show that the time resolution retrieved from the signal analysis allows to follow variations of volcanic activity at hourly time scale, thus representing a valuable source of information, in particular in areas where local geophysical observations are missing.

1. Introduction

On Earth there are about 1500 active volcanoes, most of which are not instrumentally monitored: due to the cost and difficulty to maintain instrumentation in volcanic environments, less than half of the potentially active volcanoes are monitored with ground-based sensors, and even less are considered well-monitored (Valade et al., 2019). Volcanoes can produce far-reaching hazards that extend to distances of tens or hundreds of kilometers for large eruptions, or, under certain conditions, also for smaller eruptions (Brown et al., 2017). For example, the VEI 3 eruption of Augustine Volcano, Alaska, in 2006, destroyed much of the monitoring network (Dabrowa et al., 2014); this example demonstrates the need, where possible, to monitor volcanoes from a range of distances.

Satellite remote sensing can definitely provide crucial observations when ground-based monitoring is limited or lacking (Valade et al., 2019). Volcanic eruptions are often (but not always) preceded by precursor signals which may last from a few hours to a few years, indicating

* Corresponding author at: Department of Earth Sciences, University of Firenze, via G. La Pira 4, 50121 Firenze, Italy.
E-mail address: sveva.morelli@ingv.it (R.S. Morelli).

https://doi.org/10.1016/j.jvolgeores.2022.107707
Received 18 July 2022; Received in revised form 19 October 2022; Accepted 29 October 2022
Available online 3 November 2022

a state of unrest; these signals include changes in seismicity, ground deformation, gas emissions, and/or thermal anomalies (Pallister and McNutt, 2015; Sparks et al., 2013; Phillipson et al., 2013). Apart from seismicity, all of these can be monitored from space by exploiting various wavelengths across the electromagnetic spectrum: Synthetic Aperture Radar (SAR) is widely used for the quantification of surface deformation (Pinel et al., 2014; Dzurisin, 2003), infrared (IR) for the quantification of heat radiation (Harris, 2013), and ultraviolet (UV) for the quantification of SO_2 degassing (Carn et al., 2017; Theys et al., 2019). Today, a growing number of new Earth Observation (EO) satellites is providing freely available imagery, with global coverage at unprecedented spatial and temporal resolutions: this is a game changer for volcano monitoring. In particular, the Copernicus Sentinel missions, launched by the European Space Agency (ESA), operate a range of instruments which provide the potential for a comprehensive monitoring of volcanic unrest and eruptive dynamics, opening pathways to global, multi-sensor volcano monitoring (Berger et al., 2012). However, still some limitations exist, related mostly to cloud cover, that might prevent event detection, or sampling interval, that limits satellite observations only to long term (>hours) variations of the activity.

Volcanic eruptions emit a considerable amount of acoustic energy in the infrasonic frequency band ($f < 20$ Hz) that, given the low attenuation in stratospheric waveguides (Drob et al., 2003), can be recorded from local (<15 km) to global (thousands of km) distances (e.g., Campus and Christie, 2010; Dabrowa et al., 2011; Matoza et al., 2011a; Matoza et al., 2017). Infrasound recordings allow, under favourable atmospheric conditions, detection, location (Campus and Christie, 2010) and quantification of volcanic emissions short after (tens of minutes) the event occurrence also from large distance (> several hundreds of km) observations (e.g. Fee and Matoza, 2013; Matoza et al., 2019; Marchetti et al., 2019). A number of studies have used infrasound data recorded by the International Monitoring System (IMS) of the Comprehensive Nuclear Test Ban Treaty Organization (CTBTO) for investigating volcanic eruptions worldwide (e.g. Arnoult et al., 2010; Fee et al., 2010, 2011; Matoza et al., 2011b; Fee et al., 2013; Dabrowa et al., 2014; Taisne et al., 2019; Perttu et al., 2020; Rose and Matoza, 2021; De Negri et al., 2022). Among the others, Garcés et al. (2008) showed how acoustic remote sensing may complement seismic observations and satellite remote sensing to improve continuous monitoring of wide regions of potential eruption hazard. Fee et al. (2011) reiterated the utility of using remote infrasound arrays for the detection of hazardous emissions and characterization of large volcanic eruptions, and demonstrated how, under typical meteorological conditions, remote infrasound arrays can provide an accurate representation of the acoustic source.

Indeed, Dabrowa et al. (2011) showed a limited correlation between the height of the eruption plume and the distance at which infrasonic detections can be recorded, with the furthest stations capable of detecting events located downwind, as noted also by Matoza et al. (2011a) for the Sarychev Peak eruption. This confirms the impact of atmospheric dynamics on infrasound propagation. In fact, either Assink et al. (2012) and Assink et al. (2013) suggested that infrasound observations may be used to reduce uncertainty in the knowledge of the atmospheric specifications in the upper atmosphere and to provide wind model updates.

Recently, Perttu et al. (2020) used long-range infrasound waves, recorded by the SING array in Singapore and by the IMS infrasound network, to estimate the height of volcanic plumes first for the May 30th, 2014 eruption of volcano Sangeang Api (Indonesia), and then for the January 2020 eruption of Taal volcano (Philippines). Such quantitative assessments require however the proper modelling of propagation effects in order to retrieve from the recorded waveforms the unknown acoustic source parameters of the explosion (e.g. Kim et al., 2015), as long range infrasound signals from volcanic explosions comprise source and propagation effects along the source-to-receiver path (e.g., topography, atmospheric conditions). Indeed, in order to study the 2016–2017 eruption sequence at Bogoslof volcano (Alaska), Schwaiger et al. (2020) constructed a model of the atmospheric conditions for each of the eruptive events from sea level to an altitude of 150 km to properly account for propagation effects.

Despite many studies focused already, successfully, on selected volcanic eruptions, only few studies investigated so far the long-range event detectability, over multiple years, and accounted for false alerts. Indeed, multiple sources of infrasound, including persistent microbaroms, and local turbulence overlap with observations of individual infrasound arrays, lowering the signal-to-noise ratio and limiting the potential of infrasound for long-range monitoring. Matoza et al. (2017) used the detections list of all operational IMS infrasound arrays from 2005 to 2010 to investigate the potential of identifying volcanic explosions with multiple arrays, using back-azimuth cross-bearing. This analysis, however, allowed to identify only three eruptions in six years, because of the existence of multiple sources and low signal-to-noise ratio at the arrays. More recently, Marchetti et al. (2019) used an approach based on range corrected amplitude of signals recorded by a single array to monitor low energy (VEI $\leq$2) at Etna volcano from a source-to receiver distance of ~600 km with a good reliability. Similarly, Ortiz et al. (2021) characterized the eruptive activity of Ecuadorian volcanoes at regional distances (~15–250 km ranges) with a single array using Progressive Multi-Channel Correlation array processing, and validated their study with satellite observations from the MODIS volcano detection algorithm (MODVOLC).

In this study we present the analysis of the persistent, strombolian activity at Yasur volcano (Vanuatu) between January 2008 and December 2019, from infrasound array data recorded at IS22 array in New Caledonia, at a source to receiver distance of 400 km. We discuss the potential of infrasound to follow long-term fluctuations of activity, as well as to track single explosive events, as a complementary information to thermal infrared satellite data. We first introduce Yasur volcano and its main eruptive features. Section 3 describes the data used for the study, namely the infrasonic detections recorded by the IS22 array in New Caledonia, and the array processing put in place to derive the pressure at the source of Yasur volcano; the thermal data provided by MODIS satellites is also introduced. Results from comparison between infrasound and thermal data are shown in Section 4, and are eventually discussed in Section 5 both for short and long term monitoring perspectives.

2. Yasur Volcano

Yasur volcano (19.52S, 169.42E, 361 m above sea level) is an active and persistently explosive volcano (Bani and Lardy, 2007) located on the Island of Tanna, in the Vanuatu archipelago (southwest Pacific) (Fig. 1). Its activity is typically characterized by frequent, violent strombolian explosions from multiple active vents within two main craters, driving scoria-rich emissions up to an elevation of 300–400 m above the craters and sometimes ejecting meter-sized bombs outside the crater rim, together with less frequent, but sustained, ash emissions, lasting up to 20 s and reaching heights of several hundreds of meters (Marchetti et al., 2013). Eruption rates at Yasur are high, with up to several explosions per minute (Battaglia et al., 2016; Meier et al., 2016).

This explosive activity generates high amplitude (> 100 Pa at 1 km distance) infrasound transients. Waveform characteristics, strongly asymmetric with a sharp positive peak followed by a longer lasting wavetrain, and the propagation velocity of the wavefront within the crater (Marchetti et al., 2013) suggest that the pressure wave is radiated as a supersonic blast converting to infrasound once the source-to-receiver distance increases.

Due to its persistent activity and easy access, several field works were performed at Yasur volcano during the last 20 years, focusing on the hydrothermal system and structural setting (Peltier et al., 2012) or on the geophysical description of the explosive source process (e.g. Marchetti et al., 2013; Spina et al., 2015; Battaglia et al., 2016; Jolly et al., 2017). Seismic and visual monitoring of Yasur volcano is performed by

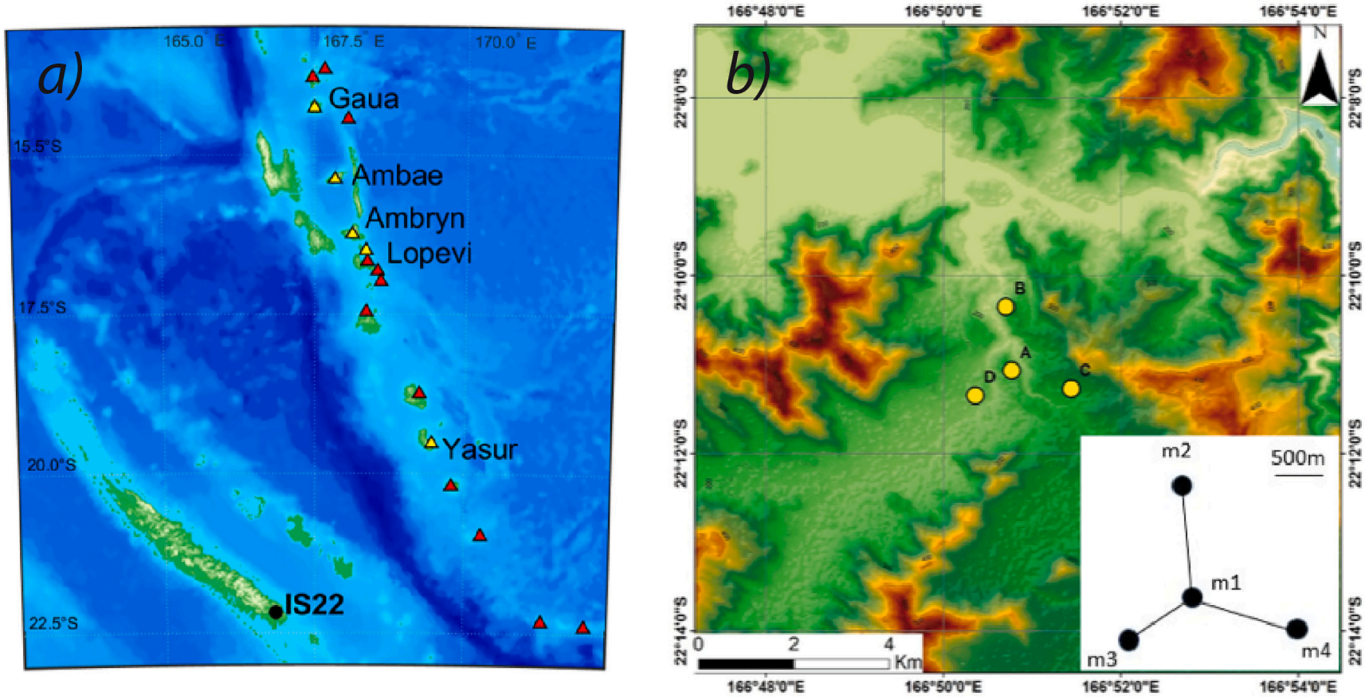

Fig. 1. Geographical map of New Caledonia and Vanuatu archipelago (a), showing the positions of the active (yellow triangles) and quiescent volcanoes (red triangles) as well as the IS22 array in New Caledonia (black dot). (b) Map showing the position of the four microbarometers part of the IS22 station. (For interpretation of the references to colour in this figure legend, the reader is referred to the web version of this article.)

the Vanuatu Meteorology and Geo-Hazard Department (VMGD), which is providing an alert level (https://www.vmgd.gov.vu), and by the Vanuatu Geohazard Observatory (VGO). However, a long-term assessment on the activity level is missing and useful information might be obtained from remote thermal and infrasound observations.

Yasur, as previously mentioned, has an overall sustained activity, with alternating periods of high or low number of explosions. The VMGD and the VGO periodically issue bulletins regarding Yasur's activity, with particular reference to the alert level (Vanuatu Volcanic Alert Level, VAAL), which ranges from 0 (insufficient monitoring to make assessment) to 4 (very large eruption, island-wide danger), as specified by the Global Volcanism Program (GVP, 2022, https://volcano.si.edu/). Due to the limited monitoring facilities, the VAAL issued by VMGD and VGO is based also on sparse direct observations of the activity; hence the need of additional monitoring solutions. Although the information in the bulletins is not comprehensive, we managed to identify the general variations of the volcanic activity level during our studied period (January 2008 – December 2019).

In August 2008 local seismic and infrasound observations showed violent Strombolian activity; as observed by Marchetti et al. (2013), the rate of infrasound transients produced by that activity was as high as one explosion per minute, with peak amplitudes exceeding 80 Pa at 1 km distance from the vent. Similar activity was documented during March, May, June, and July 2009, before a general decrease of activity starting from July 2010. In 2011, satellite images from Ozone Monitoring Instrument (OMI) and MODIS as well as seismic observations and assessments made by VGO indicated degassing and explosive activity above ordinary levels from all three active vents, starting from May, with a relative decrease in June/July. The 2012 volcanic activity was characterized by sporadic episodes in May–June, with strong explosions ejecting bombs; ash emissions were recorded in July (GVP). In 2013, a general increase of explosive activity was reported starting from April (the VAAL being 2) in agreement with a strong SO_2 emission measured in May by the OMI satellite. During 2014 and most of 2015 a long lasting period of low explosive activity was reported and the VAAL was decreased to 1, to be raised back to 2 starting from November 2015, based on VGO observations and assessments. The VAAL remained at 2 during 2016 and the activity slightly decreased in early 2017. A new increase of activity and of the alert level started since June 2017 and remained high throughout 2018 and 2019.

3. Data and method

3.1. Infrasound data recorded by I22FR array

The IS22 infrasound array (22.19°S, 166.84°E), deployed in New Caledonia (Fig. 1), is part of the global infrasound network of the Comprehensive Nuclear-Test-Ban Treaty (CTBT) International Monitoring System (Christie and Campus, 2010). Deployed in early 2000, the IS22 4-elements array has a triangular geometry with a central element, an aperture of 2.3 km and is equipped with four MB2000 microbarometers (Le Pichon et al., 2005a, 2005b). The MB2000 has been designed to operate from DC up to 27 Hz with an electronic noise level of 2 mPa RMS in the 0.02–4 Hz frequency band. In order to minimize the effect of winds, each sensor is connected to an 18-m-diameter wind noise reducing system (WNRS) equipped with 32 inlet ports that significantly improve the detection capability above 1 Hz (Alcoverro and Le Pichon, 2005). Infrasound data from the four array elements are sampled continuously at 20 Hz, with data being transmitted to the CTBT International Data Centre (IDC) in Vienna.

The array is optimally located to record data from Yasur volcano, having a source-to-receiver distance of 400 km and a back-azimuth of 42.7° respective to North. The infrasound array is also located in an ideal position to record activity from other active volcanoes in the Vanuatu archipelago. Le Pichon et al. (2005a, 2005b), showed that IS22 has continuously recorded infrasound data from Yasur volcano during the Austral summer (from September to March), when high-altitude (50 km) westward winds enhance stratospheric ducting from Yasur towards the array. This allowed to use the seasonal deviation (up to 15°) of the raypath to evaluate the real amplitude of high-altitude winds.

3.1.1. Array processing

In order to identify infrasound signal from noise, we apply the procedure described in detail by Ulivieri et al. (2011), and calculate amplitude and time delay from cross-correlation between infrasound data recorded within a given time window by all possible sensor triplets. A detection of coherent infrasound signal is defined when time residual among cross correlation time shift is minimal, below a threshold value that strongly depends on the array aperture and expected signal frequency (Garces and Hetzer, 2002). Once a detection is defined, we calculate back-azimuth (B_{az}) and apparent velocity (c_a) from the time shift of the signal recorded at the different array elements, as well as amplitude (*Prs*) and peak frequency (*Fp*) of delay and stacked infrasound signal.

The propagation back-azimuth indicates the direction where the infrasound wave is coming from and is related to the location of the source. The apparent velocity is the velocity the wave would have if it would propagate in the same plane as defined by the array: it is linked to the incident angle of the infrasound wave (γ) and, therefore, to the altitude of the source (Ulivieri et al., 2011) or to the returning height in case of long range propagation in atmospheric ducts (Le Pichon et al., 2005a,b). With a sampling rate of 20 Hz, the expected resolution at 1 Hz is of the order of 0.5° for the azimuth and of 5 m/s for the apparent velocity (Le Pichon et al., 2005a, 2005b).

The array processing adopted here provides the same basic wavefront properties (B_{az}, c_a, *Prs*, *Fp*) provided by the Progressive Multi-Channel Correlation (PMCC) algorithm (Cansi, 1995) adopted already in many studies (Le Pichon et al., 2005a, 2005b; Le Pichon et al., 2010; Matoza et al., 2011b; Ortiz et al., 2021; De Negri et al., 2022), or by the open-source multiple sequential narrow-band least-squares processing tool for infrasound array data presented by Iezzi et al. (2022). It differs however from these algorithms, as we consider infrasound data in a single frequency band and a fixed time window of analysis, that are chosen according to the signal of interest and the desired time resolution.

In agreement with the peak frequency of infrasound detections from Yasur and identified at IS22 array with broadband PMCC analysis by Le Pichon et al. (2005a, 2005b), our multichannel correlation analysis is applied to infrasound data, band-pass filtered between 1 and 3 Hz. To describe the long-term (months/years) variations of infrasound signal recorded at the array we consider a time window of 60 s with a time shift of 10 s (Fig. 2). The analysis, providing a total of 565,177 detections (137 detections/day), highlights a marked seasonality: infrasound detections with peak pressure of 0.3 Pa at the array are mostly recorded during the Austral summer (between September and March), when westward propagation is enhanced in the southern hemisphere by stratospheric winds. Detections are showing a recurrent back-azimuth of 37–49°N (Fig. 2b), and apparent velocity < 360 m/s (Fig. 2c), which are in good agreement with infrasound propagation through the stratospheric duct from Yasur volcano, positioned at the real back-azimuth of 42.7°N from IS22. Two major gaps in the analysis are reported for April–June 2011 and between August 2017 and February 2018, probably due to temporary malfunctions of the array.

The window length used for the cross-correlation analysis strongly controls the analysis time resolution, and prevents to discriminate discrete transient events spaced in time less than the selected time window itself. Here, while Fig. 2 can be used to describe the long-term variation of explosive activity at Yasur volcano, mostly in terms of the recorded maximum amplitude, it might not properly reflect the rate of explosive events, that was observed from local infrasound investigations to be high as several events per minute (Battaglia et al., 2016; Meier et al., 2016).

In order to test the potential of long-range infrasound for detecting events closely (<1 min) spaced.

in time, we applied the multichannel correlation analysis to band pass (1–3 Hz) filtered infrasound recorded.

over 10 s long time windows with a time shift of 1 s (Fig. 3). Detections obtained between February 16th, 2014 and February 18th, 2014 show a signal amplitude that is highly modulated through time as a function of local noise at the array, that strongly reduces during the night (between 06 and 19 UT) when the signal-to-noise ratio increases and signals from Yasur volcano are recorded. Zoom into 1.5 h of data (Fig. 4) shows that infrasound from discrete transient events, with the back-azimuth consistent with Yasur volcano, can be clearly identified and suggests occurrence of discrete explosive events repeating every 2–10 min. This is used to compute the number of explosions (reaching the maximum of 20) per hour over the day-long sample period (Fig. 3).

3.1.2. Filtering of infrasound detections

An infrasound transient is recorded at a distant array as a long-lasting signal that will be identified following the array processing described in Section 3.1.1 as a cluster of detections closely spaced in time. These might show a trend or variation in back-azimuth and/or apparent velocity, according to the various ray-paths reaching the station, but will be characterized by a persistency through time.

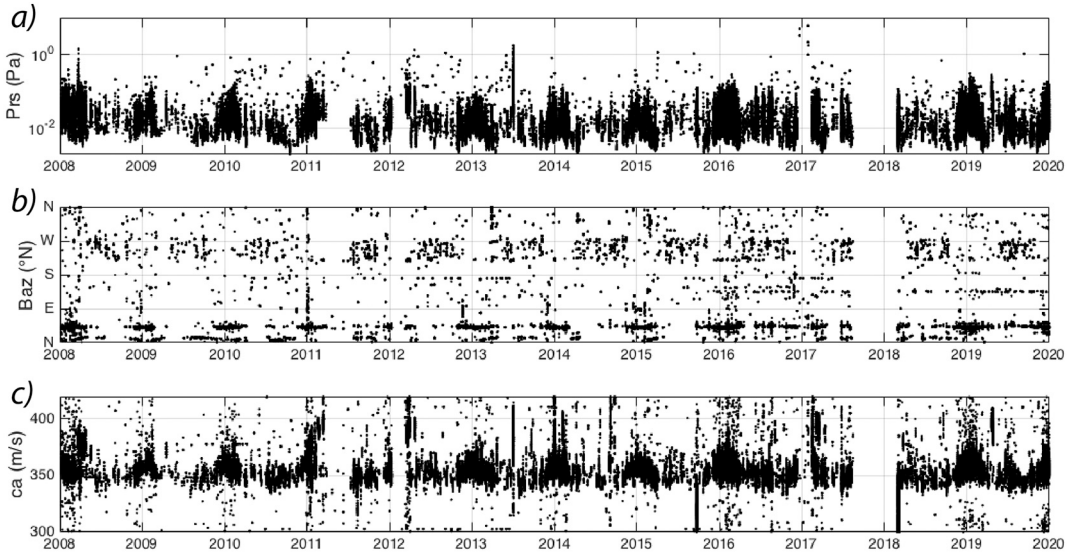

Fig. 2. Pressure amplitude (a), back-azimuth (b) and apparent velocity (c) of infrasound detections at IS22 infrasound array in the 1–3 Hz frequency band. The dominant azimuth corresponds to the Yasur volcano – IS22 direction (42.7°N).

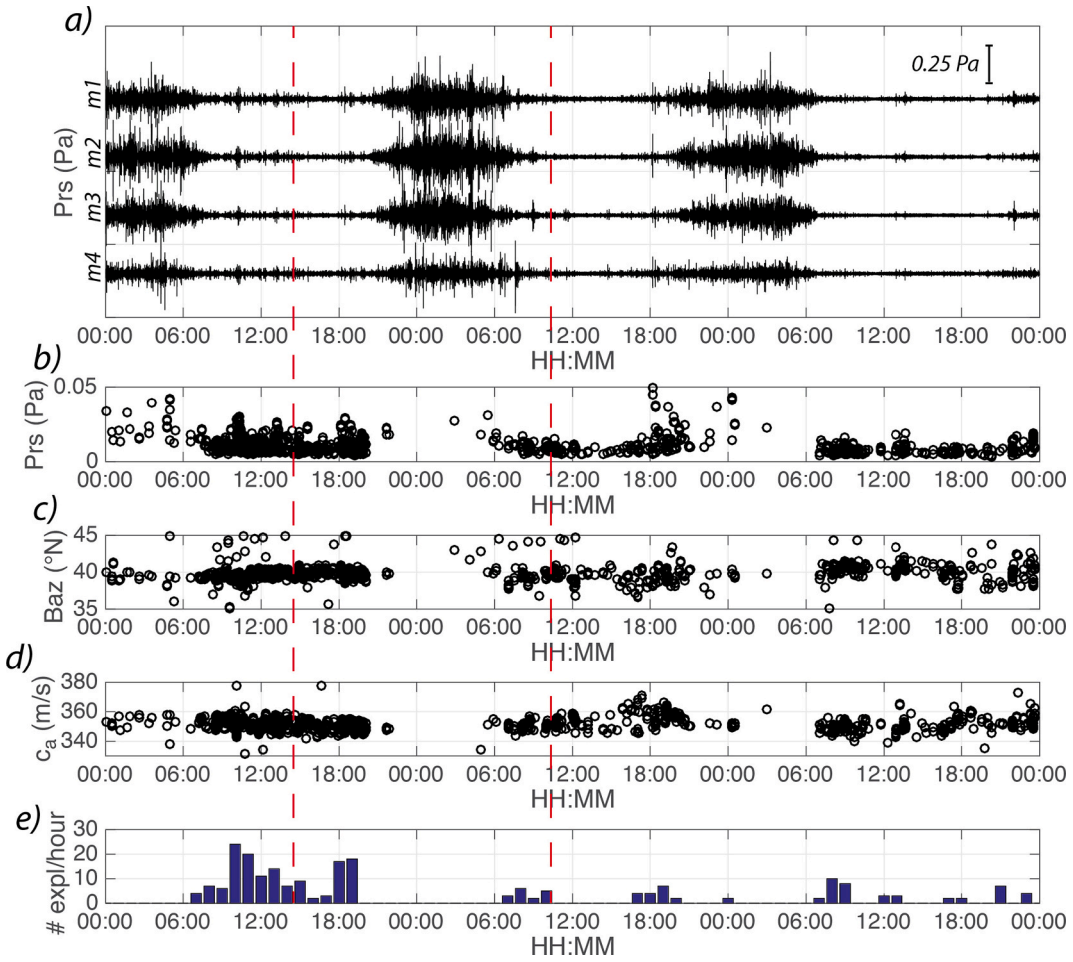

Fig. 3. Bandpass (1–3 Hz) infrasound data recorded by the 4 elements of the IS22 infrasound array for February 16th, 2014 and February 18th, 2014 (a). Amplitude (Prs, b), back-azimuth (Baz, c), apparent velocity (c_a, d) of infrasound detections at the array calculated condiering a time window of 10 s and a shift of 1 s. Number of explosions/h inferred from long range detections (e). Red lines represent the recording times of MODIS infrared thermal images. (For interpretation of the references to colour in this figure legend, the reader is referred to the web version of this article.)

In order to identify and extract infrasound detections related to the persistent explosive activity of Yasur volcano we first grouped clusters of detections into discrete events and then extract only events coming from the direction of the volcano. We considered only groups of >6 detections, with a maximum 30 s time difference between successive detection tolerated. Considering the processing parameters of 60-s-long time window of analysis and 10-s of shift, this corresponds to signals lasting >1 min. Shorter-duration events at the array, that are likely not consistent with any infrasound signal propagating from large distances, are therefore removed from the long-term array analysis of explosive activity presented in Fig. 5.

The azimuthal filtering of detections was applied considering solely detections that are recorded at the array within a 10-degree tolerance from the real back azimuth to the volcano (B_{az} = 42.7° +/− 10° respective to N). This azimuthal interval allowed accounting for errors and propagation effects deviating the ray propagation in the atmosphere, while removing detections coming from different directions. The azimuthal tolerance was chosen in accordance with a previous result by Le Pichon et al. (2005a, 2005b), that showed the marked variability of back-azimuth of infrasound from Yasur recorded at IS22 (Antier et al., 2007), in good agreement with modeled azimuthal deviation due to the seasonal reversibility of the zonal stratospheric wind.

Fig. 5 shows that propagation is not only affecting the detectability of the signal, but also the wave parameters, such as back-azimuth, apparent velocity and pressure amplitude recorded during the Austral summer. Maximum values of pressure amplitude (>10^{-1} Pa) are recorded at the array between January and February, with lower values of back-azimuth (40–42°N) and higher apparent velocity (370–380 m/s). From March to November, pressure amplitude (between 10^{-1} and 10^{-2} Pa and < 10^{-2} Pa) and apparent velocity (340–350 m/s) tend to be lower while the back-azimuth tends to be larger (43–45°N).

3.1.3. *Retrieving the pressure at the source*

The arrival times, back-azimuth and apparent velocity of pressure waves recorded by infrasonic arrays allow the location of explosive sources that detonated in the atmosphere, but infrasound propagation is not constant in all directions, as it follows the dynamics of the atmosphere: there is significant spatial and temporal variability in the physical properties of the atmosphere (Drob et al., 2003). A full description of infrasound propagation would then require the knowledge of the dynamical atmosphere from the ground to the thermosphere (up to 150 km), combining numerical weather prediction models with empirical models of the temperature and wind in the upper atmosphere (Schwaiger et al., 2019), in order to compute a 3D ray-tracing to define the real path of the infrasonic ray and to eventually infer the pressure amplitude at the source. However, for the specific case of infrasound produced by Yasur volcano, Le Pichon et al. (2005a, 2005b) showed that the majority of infrasound energy recorded at IS22 array is actually confined within the stratospheric duct with a maximum returning height of 40–50 km.

For the purpose of this study, atmospheric propagation effect is described using ECMWF data (http://www.ecmwf.int/). ECMWF global-

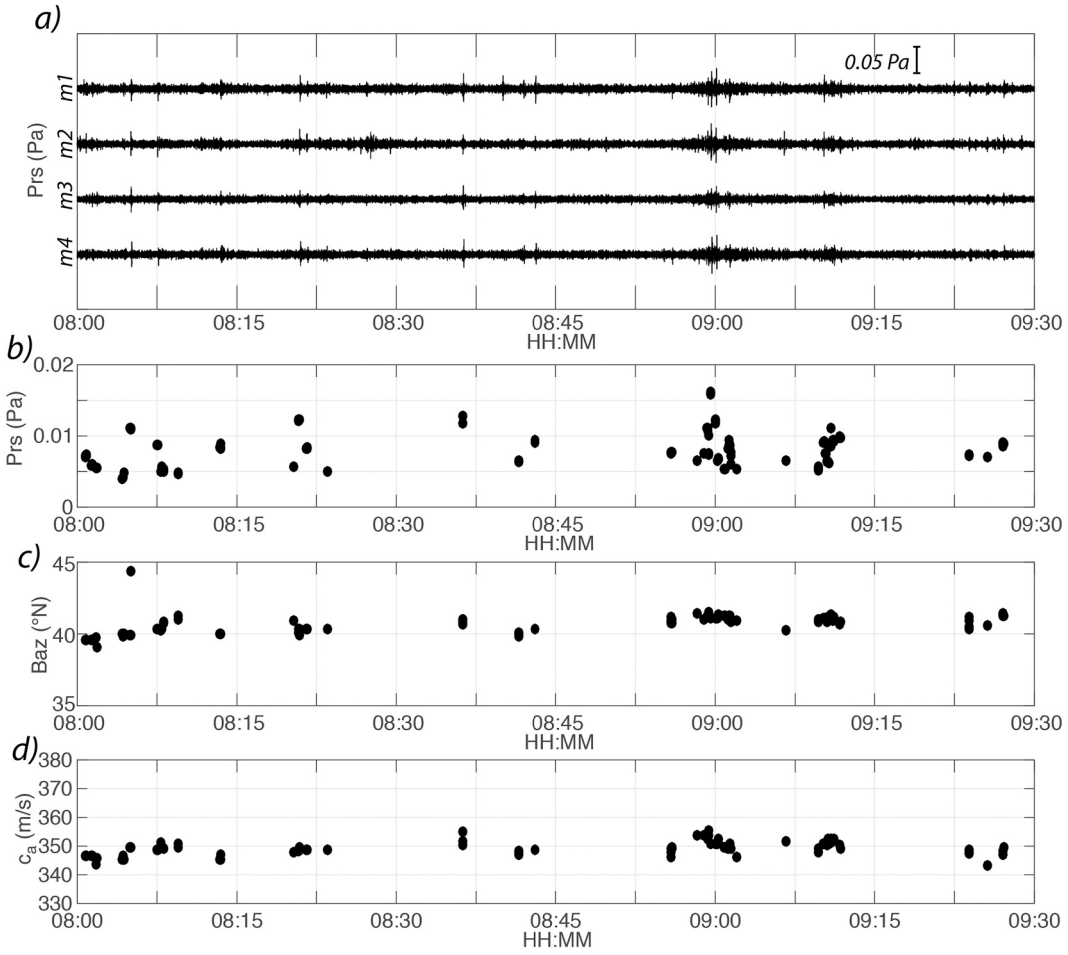

Fig. 4. Same as Fig. 3a-d, but zoom into data recorded between 08:00 and 09:30 UT on February 18th, 2014, showing discrete explosions recorded at the array and identified as discrete clusters of infrasound detections. Bandpass (1–3 Hz) infrasound data recorded by the 4 elements of the IS22 infrasound array (a). Amplitude (Prs, b), back-azimuth (Baz, c), apparent velocity (c_a, d) of infrasound detections.

scale GRIB ERA-Interim data were retrieved for each month, with a horizontal resolution of 1°, for a time period between 2008 and 2019. We retrieved all the relevant parameters (temperature, humidity, horizontal wind speed and pressure) and computed the effective sound speed (the adiabatic sound speed summed to the wind component along the ray-path) for an infrasound wave radiated from Yasur volcano and recorded at IS22 array.

In this study we adopt for simplicity the effective sound speed ratio ($C_{eff\text{-}ratio}$, Fig. 6b), defined as the ratio between the effective sound speed calculated at a given altitude and the sound speed at the ground level (Le Pichon et al., 2012), as the most relevant parameter to study wave propagation When the effective sound speed at a given altitude exceeds the velocity at ground level ($C_{eff\text{-}ratio} > 1$), a return of infrasound energy to the ground is expected due to refraction. This might lead to ducting of infrasound waves in atmospheric waveguides, where attenuation is minimal, making infrasound propagation more efficient.

For this specific case, being infrasound from Yasur recorded at IS22 due to stratospheric ducting (Le Pichon et al., 2005a, 2005b), we calculate the $C_{eff\text{-}ratio}$ considering the maximum C_{eff} expected at an altitude between 30 and 60 along ray propagation and the one at the ground. For distances of >200 km this approach predicts two main scenarios: (I) upwind propagation, when $C_{eff\text{-}ratio} < 1$: thermospheric paths dominate (no stratospheric ducting); (II) downwind, when $C_{eff\text{-}ratio} > 1$: atmospheric conditions enable long-range propagation through the stratospheric waveguide, with stratospheric arrivals being recorded as first arrivals (Le Pichon et al., 2012; Tailpied et al., 2016). $C_{eff\text{-}ratio}$ at Yasur volcano, in the direction of propagation towards IS22 array, is usually >1 from mid-November to mid-March due to the favourable winds, while it is smaller than 1 from mid-March to mid-November due to the winds blowing against the source-to-receiver direction of propagation (Fig. 6). This explains the seasonal variation of infrasound detections at the station (Fig. 5).

To calculate the expected attenuation of infrasound waves, we used the equation of Le Pichon et al. (2012), where attenuation is a function of frequency (f), distance between the source and the array (R) and effective sound speed ratio ($C_{eff\text{-}ratio}$). In our case, the distance of 400 km between Yasur and IS22 and an average frequency of 2 Hz were considered. This is in agreement with the frequency content of infrasound from Yasur recorded at IS22 (Le Pichon et al., 2005a, 2005b) and allows to enhance stratospheric arrivals that are typically characterized by the largest amplitude in the high frequency band (1–5 Hz), where the amplitude of persistent coherent signals, such as microbaroms, is basically absent (Pilger et al., 2018). The attenuation is generally low (−50 dB) between the beginning of November and the end of March of each year, while it reaches about −90 dB during the Austral winter between April and October (Fig. 6).

Fig. 6 shows the range of corrected infrasonic amplitudes at Yasur volcano during the whole period of analysis, accounting for propagation effects derived from real atmospheric conditions between the volcano and the IS22 array at the time of the event. It is obtained by dividing the amplitude of infrasound detections (Fig. 2a/Fig. 6a) for the attenuation derived for infrasound waves propagating through the stratospheric duct (Fig. 6c) when the C_{eff_ratio} is larger than 1 and a stable duct is present. For any time, the development of a duct is not expected (C_{eff_ratio}

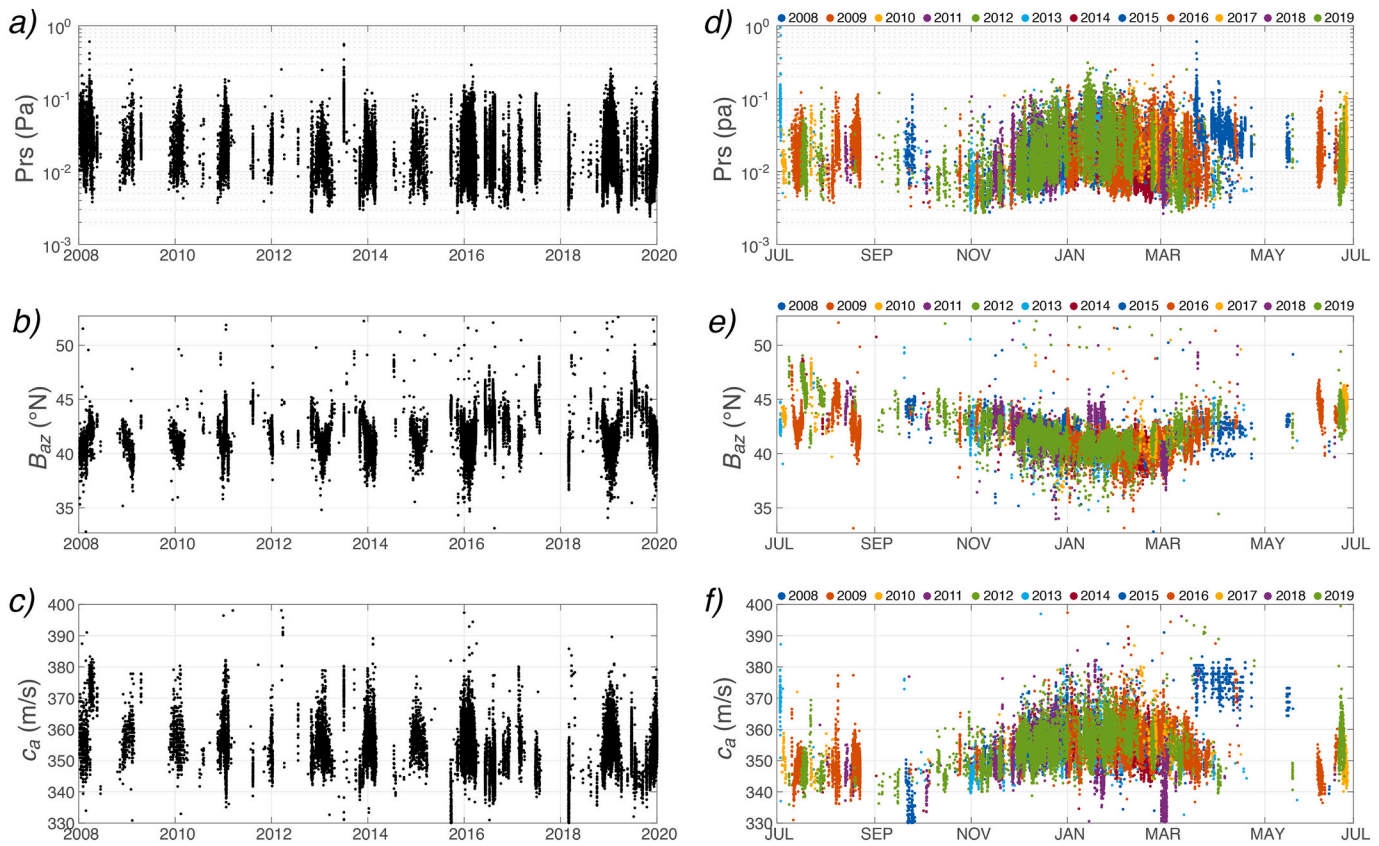

Fig. 5. Amplitude (a, d), back-azimuth (b, e) and apparent velocity (c, f) of infrasound detections at the IS22 infrasound array in the 1–3 Hz frequency band and extracted according to detection clustering and azimuthal filtering in order to reflect possible infrasound radiated by Yasur volcano, shown over the entire observation period (left) and plotted as a function of day of the year (right).

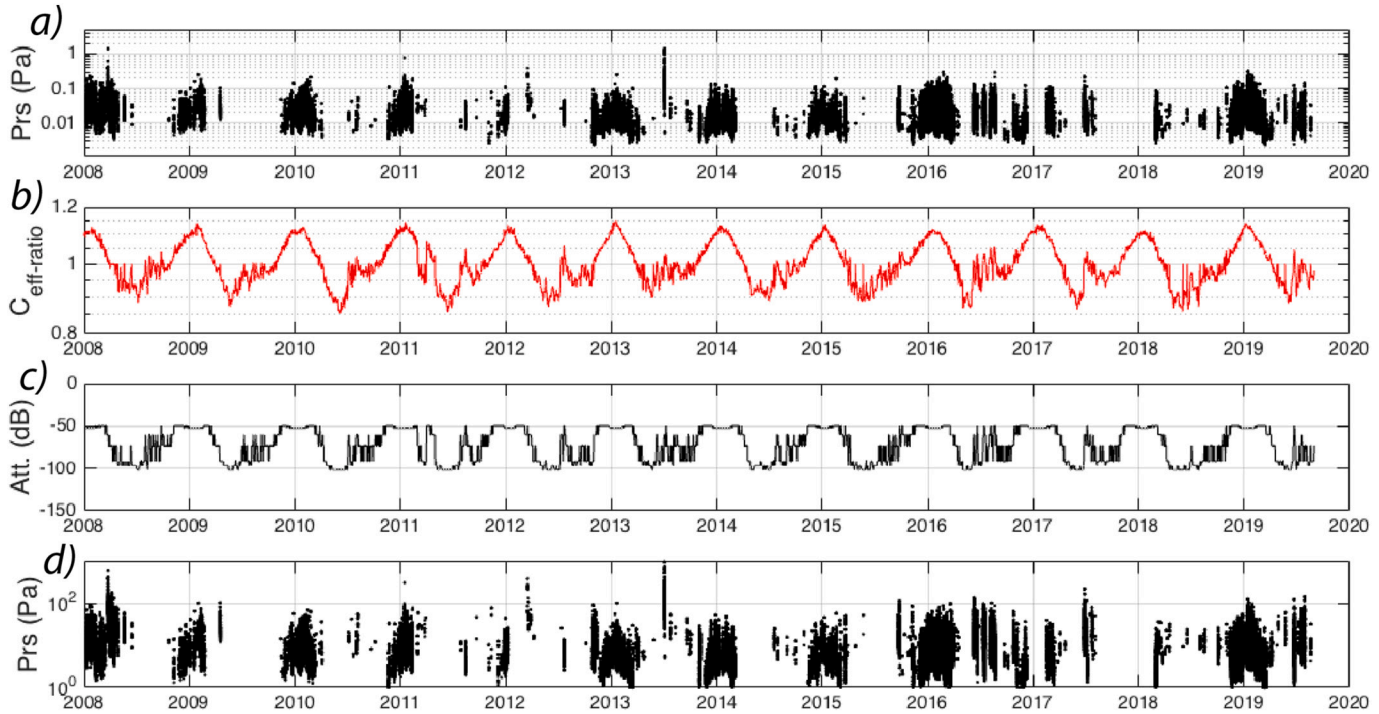

Fig. 6. Pressure amplitude registered at the IS22 array (a), Effective sound speed ratio C_{eff_ratio} (b) and attenuation (c) calculated from ECMWF ERA-Interim data by applying the equation proposed by Le Pichon et al. (2012) for a source-to-receiver distance of 400 km and a frequency content of 2 Hz. (d) Range-corrected pressure of infrasound signals produced by Yasur and recorded at the IS22 array.

< 1), the attenuation of the direct wave is applied (− 60 dB). This allows to limit overestimating signals recorded during upwind propagation conditions, that might actually results from additional sources than Yasur or reflect unusual propagation conditions that are not entirely described by the NWP model. The pressure amplitudes recorded by the IS22 array are below 1 Pa for all the periods taken under consideration, whereas the range corrected amplitudes span two orders of magnitude, between few Pa to ~100 Pa.

3.2. Space-born thermal infrared data, MIROVA

Space-borne thermal infrared observations are routinely used to evaluate and monitor volcanic activity at large scale. Thermal data provide information about the presence, or absence, of thermal anomalies (i.e., hotspots) associated with the observed phenomena (Ramsey et al., 2012; Harris, 2013) and generally allows deriving information on: (I) the location of the hotspot(s), (II) the area and temperature of the heat source, (III) the excess of radiance or heat flux, and (IV) the mass or volume flux.

The ElectroMagnetic (EM) radiation with wavelengths longer than those of visible light is called InfraRed (IR) radiation. This range of emissions spans from 0.74 μm to 250 μm and includes the thermal radiation emitted by the volcanic products, such as lava and hot ash. The most useful spectral regions for observing the thermal signature of volcanic bodies are those between 1.4 and 12 μm, subdivided in three main atmospheric windows: SWIR (Short Wave InfraRed; 1.1–3 μm), MIR (Middle InfaRed: 3–5 μm), and TIR (Thermal InfraRed: 8–13 μm). Among these, the MIR radiation shows the lowest attenuation levels by the atmosphere (resulting from absorption by gases and scattering by particles, wavelength dependent) and is commonly used by the main hotspot detection systems.

Geostationary and polar satellites provide infrared data with different spatial and temporal resolutions. Spinning Enhanced Visible InfraRed Imager (SEVIRI) on board of Meteosat Second Generation (MSG) satellites, for example, provides thermal data every 15 min, with a resolution of >4 km. On the contrary, sensors such as MODIS, mounted on board NASA's Terra and Aqua polar satellites, acquire data approximately four times per day (2 daytime and 2 nighttime) with a spatial resolution of 1 km. Terra's orbit around the Earth is timed so that it passes from north to south across the equator in the morning, while Aqua passes south to north over the equator in the afternoon (extracted by MODIS, NASA). Some higher resolution sensors such as Landsat 8 or ASTER instead provide TIR images at resolutions of ~100 m, but with return times generally longer than a week.

Several efforts have been made to provide a near-real time monitoring system of volcanic activity based on space-borne thermal infrared data provided by MODIS satellites, such as MODVOLC (Wright et al., 2002) and Middle InfraRed Observation of Volcanic Activity (MIROVA) (Coppola et al., 2016a); its temporal frequency makes these observations perfect for monitoring any activity on land. The data have a variety of resolutions: a wide spectral range (0.42–14.24 μm), 1–2 days in time, and a high spatial resolution channel (250 m, bands 1–2; 500 m, bands 3–7; 1000 m, bands 8–36) (Khan et al., 2009; Zhang and Reid, 2009; Acharya and Sreekesh, 2013).

In this study we use MODIS nighttime data (2 nighttime images/day), elaborated by MIROVA algorithm which proved useful for detecting Yasur's thermal activity associated to the repeated strombolian explosions (Coppola et al., 2016b).

Fig. 7 shows the Volcanic Radiative Power (VRP, in Watt) for Yasur volcano, which is calculated from the radiance of pixels with thermal indexes anomalously high with respect to the background and therefore depends both on the areal extension and the amplitude of the thermal anomaly. We limit our analysis to nighttime, which is unaffected by solar heating and reflection processes and thus allows a more inclusive interpretation.

Fig. 7a shows that the measured VRP between 2008 and 2019 varies 3 orders of magnitude from 2×10^5 to 2×10^8 W (mean 2×10^7 W, std. $= 2 \times 10^7$ W). In total 1976 thermal anomalies are detected, roughly corresponding to 0.45 alerts/day, or between 10 and > 20 detections every month (Fig. 7b). In general, the sustained number of alerts/month and the persistent values of the VRP are suggesting a persistent volcanic activity through time.

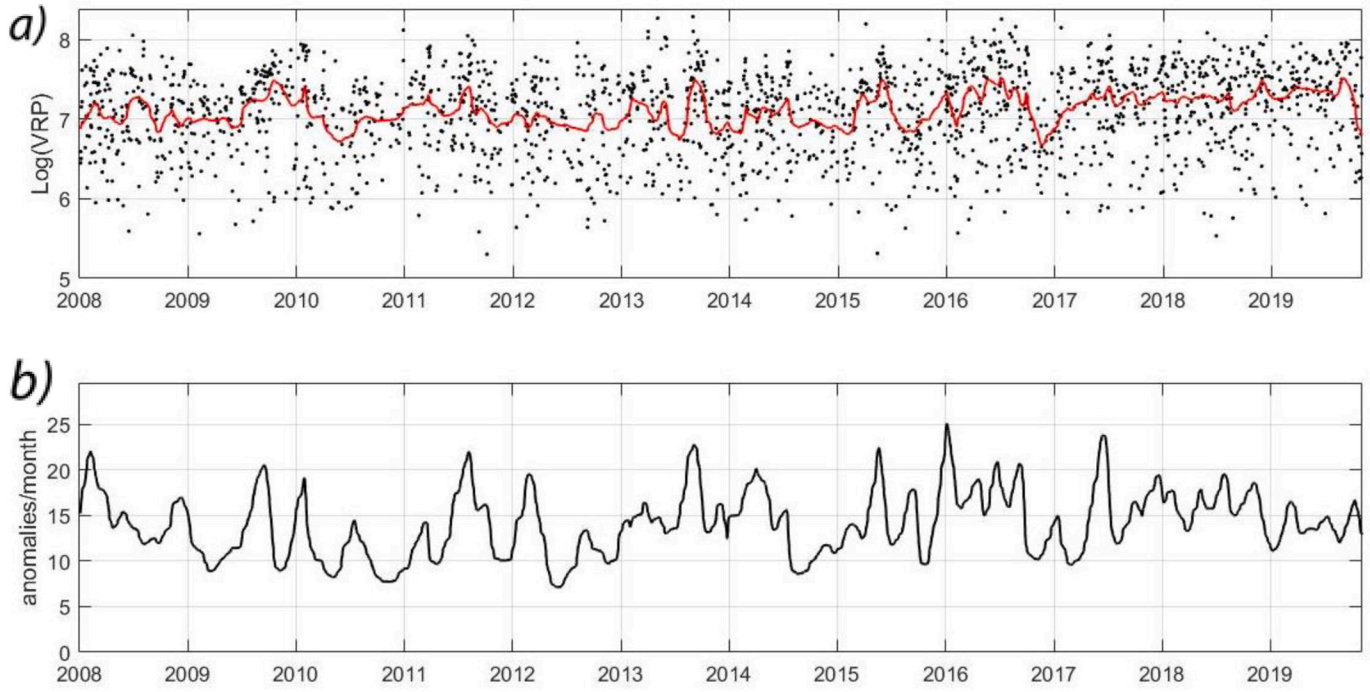

Fig. 7. Volcanic Radiative Power (a) of thermal anomalies calculated at Yasur volcano by MIROVA between January 2008 and November 2019. The red line shows the median value of thermal anomalies over a time period of one month. (b) Number of thermal anomalies detected by MIROVA each month. (For interpretation of the references to colour in this figure legend, the reader is referred to the web version of this article.)

4. Results

In order to evaluate long-term variation of explosive activity at Yasur volcano, we computed the Infrasound Parameter (IP) as defined by Ulivieri et al. (2013) and modified by Marchetti et al. (2019), for long-range infrasound propagation. The IP (IP = Ndet · Prs) is defined as the product between the mean infrasonic amplitude (Prs) and the number of detection with a back-azimuth consistent with Yasur volcano recorded in a given time window (Ndet) (Marchetti et al., 2019). It is strongly related to the persistence of the infrasound signal and increases with the number of detections per minute and with excess pressure (Ripepe et al., 2018) Fig. 8a shows the maximum, range-corrected infrasound pressure amplitude, calculated every 6 h, from range corrected detections (Fig. 6d), the normalized number of detection (Ndet, Fig. 8b) and the corresponding IP (Fig. 8c). The normalized number of detections (Ndet, Fig. 8b) varies between 0 and 60, peaking when signal from Yasur volcano is recorded continuously through time (Marchetti et al., 2019). Ndet is below 5 the 8% of the time, while it increases up to >20 the ~30% of the time, mostly in 2014 and from 2016.

From Fig. 8 it is clear that despite infrasound observations are basically absent during the Austral winter due to high attenuation of infrasound waves (Fig. 6), both the IP and Ndet suggest a relatively lower intensity of explosive activity of Yasur between 2009 and 2013, a relative peak of activity in 2014 and an increased level of activity starting from the end of 2015 that persisted until the end of our observation period.

Similarly to the VRP (Fig. 7a), the IP (Fig. 8c) appears quite persistent through time, in agreement with the sustained Strombolian activity reported for Yasur and discussed in Section 2. A better comparison on the long-term can be obtained from the cumulative amplitude of the two parameters that highlights better than raw data the variation in the rate of event occurrence in terms of cumulative distribution's slope. Fig. 9 shows the superposition of cumulative radiated heat energy from Yasur volcano (black) and cumulative IP (red) calculated between January 2008 and December 2019; both curves are calculated on a weekly average of the values. We used here the cumulative curve of thermal energy radiated weekly from Yasur, calculating the average weekly VRP and multiplying it by the number of seconds in a week. The curve thus obtained is in Joule, not Watts. Differently from the heat energy, that is continuous through time, the IP is not defined during unfavourable propagation conditions (i.e. from April to October), and its cumulative distribution is therefore highly discontinuous.

While infrasound is a direct consequence of the pressurized volcanic gas released in the atmosphere, able to drive magma fragments and ash within a volcanic plume, thermal infrared energy reflects the presence of hot material and might arise not only from the hot ash and lapilli injected in the atmosphere and accumulating nearby the vents, but also from the presence of a lava lake or flow without infrasound energy being radiated (Coppola et al., 2012). For the specific case of Yasur volcano both cumulative datasets share a common trend and are characterized by distinct slopes that increase from 2008 to 2015 to 2016–2019, thus indicating a general increase of activity, both in terms of infrasound and thermal energy, starting from the beginning of 2016. This conclusion is in general agreement with the activity level inferred from GVP and VGO observations and assessments (Section 2).

5. Discussion

Results presented in this study show that array observations of infrasound signal radiated by Yasur volcano and recorded at IS22, at a source-to-received distance of 400 km, can be used both to quantify the long-term (multi-year) variations in the intensity of its persistent explosive activity, and to provide, during favourable propagation conditions and low noise periods at the array, a timely description of the explosive activity, such as the time of occurrence of the discrete events and their range corrected excess pressure.

5.1. Long period monitoring

Despite affected with uncertainties, remote infrasound observations are particularly useful for Yasur volcano, as its persistent explosive activity fluctuated through time between low- and high-intensity explosions, but without clear trends highlighted from reports or local observations. Here, long-term remote infrasound records, in general

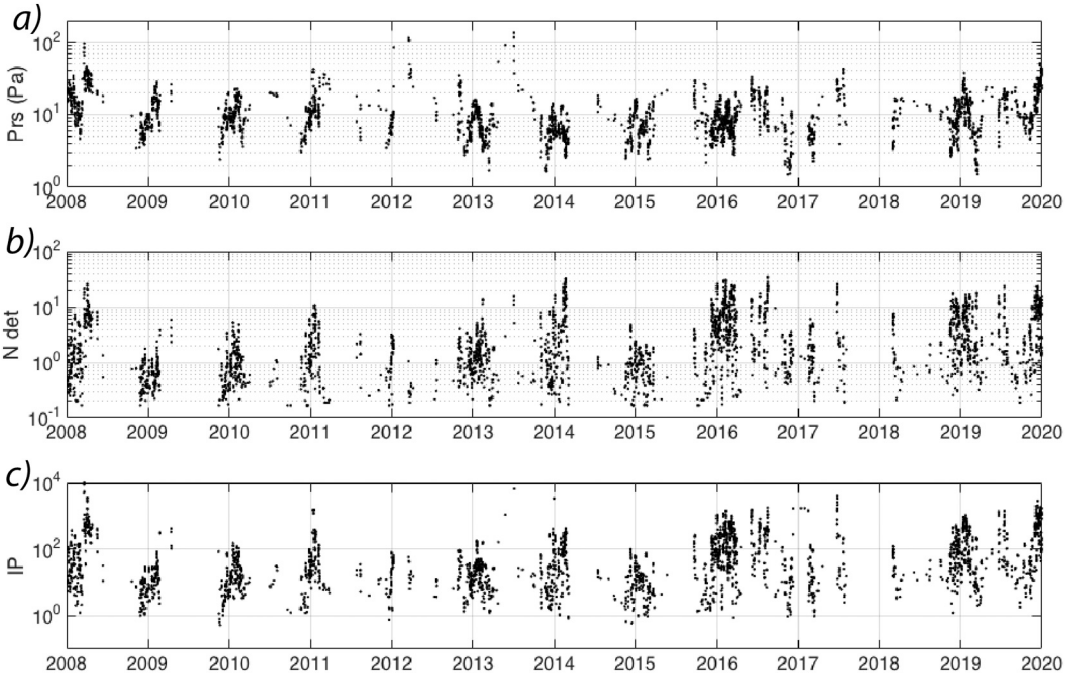

Fig. 8. Range corrected mean infrasound amplitude (a), normalized number of detections (b) and Infrasound parameters (c) calculated every 6 h for Yasur volcano over the whole observation period.

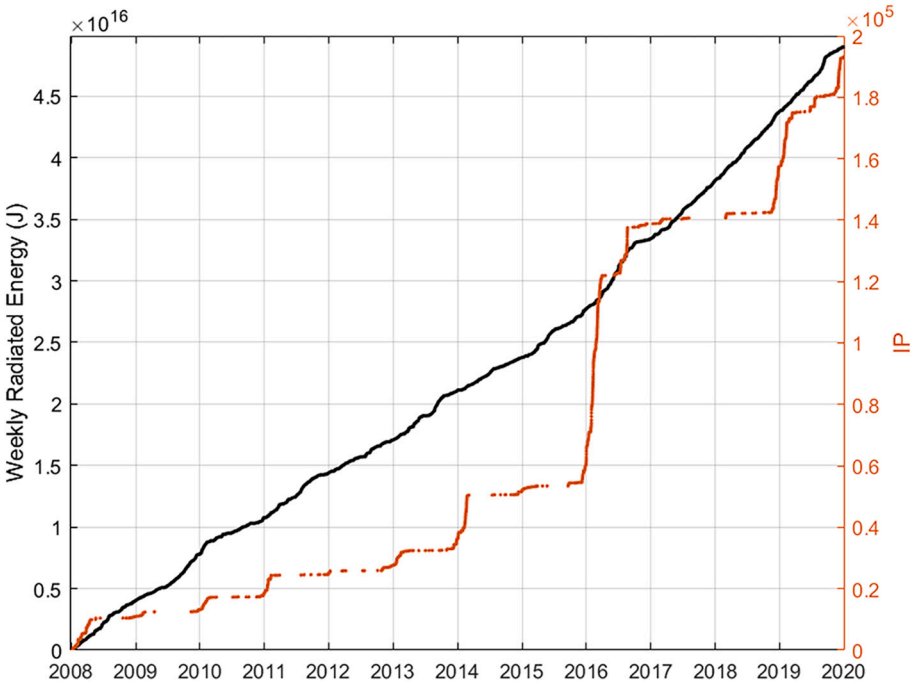

Fig. 9. Cumulative Infrasound Parameter (orange) and cumulative weekly radiated heat energy in Joule (black) for Yasur volcano in the period January 2008 – August 2019.

agreement with space-borne infrared thermal imagery suggest a clear increase of explosive intensity after 2016 (Fig. 9).

Presented results highlight however how seasonal propagation effects (Fig. 6) and noise at the array (Fig. 3) might strongly limit the efficiency of long-range infrasound for the detection of volcanic activity (e.g. Fee et al., 2011; Ortiz et al., 2021; De Negri et al., 2022).

An additional limitation relies in the ability to properly correct pressure recorded at a distal array for propagation effects. Fig. 5 clearly shows that recorded infrasound amplitude at the array (at 400 km from the source) is approximately constant between November and April, when stable high altitude winds facilitate propagation of infrasound from Yasur to the array, while it appears to be systematically lower around the equinoxes. Once corrected for propagation effects, this trend remains (Fig. 6d), suggesting that atmospheric models around the equinoxes are less able to properly reflect the real atmospheric conditions, or that the amplitude correction adopted here for calculating the attenuation is underestimating the real effect (Le Pichon et al., 2012). This aspect is particularly important for our study, that focuses on persistent explosive activity of low intensity, while it is less critical for higher energy explosive eruptions. Nevertheless, the use of the IP parameter (Fig. 8), that combines both the range corrected pressure and the persistency of the signals, allows to minimize such effect, and provide more reliable results for a long-term (multi-years) assessments, as shown by the general agreement between the IP and the thermal activity (Fig. 9).

5.2. Short period monitoring

Although long-range infrasound is strongly controlled by propagation effects (Fee et al., 2011; Le Pichon et al., 2012) and is, therefore, commonly usable only during specific time periods, results presented in this study shows that it is very efficient to follow short-term variations. The high temporal resolution of infrasound data, compared to satellites infrared thermal data, allows to distinguish between subsequent explosions and to follow the real explosive activity in near-real time. This is clearly demonstrated by Fig. 4, which shows waveforms recorded at the four microbarometers of the IS22 array (a), as well as amplitude (b), back-azimuth (c) and apparent velocity (d) of infrasound detections at the array between February 16th, 2014 and February 18th, 2014, produced by discrete explosive events at Yasur volcano. This allows to evaluate variations in the intensity of discrete explosive events, in terms of amplitude at the source, as well as to evaluate the number of explosions per hour almost in near-real time and with a delay of approximately 20 min, due to the source-to- receiver propagation time (400 km) with a mean celerity of stratospheric arrivals of 320 m/s.

Due to the low amplitude of infrasound waves generated by Yasur explosions and recorded at IS22 and after undergoing high attenuation along the source-to-receiver path, the main limitation of such approach is linked to the noise levels at the array (Dabrowa et al., 2014). From Fig. 3 it is evident that during the local daytime (19:00–06:00 UTC) the noise is too high and completely overlaps with the infrasound transients produced by Yasur explosions. At night time, when the noise at the station reduces and the signal-to-noise ratio increases, infrasound signals from volcanic explosions are more clearly detected and allow identification of individual explosive episodes.

From the same figure, however, we see how the MODIS thermal infrared data used to obtain the VRP and the thermal energy is flawed in its short-term monitoring (red lines in Fig. 3) due to the sparse sampling time of satellite-borne imagery. Having an anomaly every one or two days, the VRP takes a picture of the situation at that precise moment, but it is not able to give information about the short-term (minutes/h) activity of the volcano.

5.3. Implementation of operational monitoring solutions

Infrasound stations located at regional or global distances from active volcanoes cannot replace local monitoring networks, that provide an all year-round detailed description of volcanic activity with high time resolution. Nevertheless, long-range infrasound has the potential of providing quantitative information on explosive volcanic activity, even of low energy.

As discussed in detail, such an approach requires however to integrate array processing of infrasound data, necessary to identify volcanic infrasound from additional sources, with atmospheric studies, required

to correct pressure recorded at the array for propagation effects. In the specific case of Yasur volcano, previous analysis of broadband infrasound array observation and propagation modelling (Le Pichon et al., 2005a, 2005b) allowed us to rule out thermospheric arrivals, and we therefore computed the expected attenuation simply accounting for the C_{eff_ratio} within the stratospheric duct. However, extrapolation of such an approach would require modelling the full 3D ray propagation to properly estimate the real signal attenuation.

Additionally, presented results clearly show that for the specific case of Yasur volcano and IS22 array, long-range infrasound is almost completely prevented during unfavourable propagation conditions, as infrasound energy is largely attenuated and therefore not discernible. This depends both on the mostly East-West mutual position of the volcano and the array, strongly affected by stratospheric jets, and on the limited energy of the source. For Yasur volcano this limitation might be reduced with an additional infrasound array east of the Vanuatu archipelago, in order to record signals when the IS22 array is operating under unfavourable wind conditions. Several network performance studies (Tailpied et al., 2016, 2022) focused specifically on this topic and should be considered when considering the potential of long range infrasound for volcano monitoring.

For example, Assink et al. (2013) uses a set of two arrays for the study, integrating observations coming from satellites, which might be affected by lack of high-resolution data, in particular in areas where the deployment of local monitoring networks is difficult or impossible. This might contribute significantly to the monitoring and hazard assessment of many volcanoes around the world.

6. Conclusions

In this study we showed that long-range (> several hundreds of km) infrasound monitoring is possible and efficient, in the context of remote volcano monitoring, but only during favourable propagation conditions in the volcano-receiver direction. We analysed twelve years (January 2008 – December 2019) of infrasound data recorded at the IMS IS22 infrasound array in New Caledonia, in order to investigate infrasound radiation by persistent Strombolian explosive activity at Yasur volcano located on Tanna Island (Vanuatu) at a source-to-receiver distance of 400 km from the array.

During periods of low noise at the array, discrete infrasound transients related to explosive events at Yasur volcano were recorded in New Caledonia and allowed to evaluate monitoring parameters such as the intensity of explosive events and the number of events per hour. The time resolution of long-range infrasound is comparable with local monitoring systems and is exceeding significantly the one of satellites, but is limited to specific time periods, when propagation from the source to the receiver is favourable and the noise levels at the array are low.

The use of long-range infrasound strongly depends on the possibility to account for propagation effects. In the specific case of Yasur volcano and IS22 array, infrasound energy is almost entirely confined to stratospheric ducts (Le Pichon et al., 2005a, 2005b), that enhance propagation between November and April. Infrasound detections from Yasur at IS22 are almost missing otherwise, despite persistent explosive activity is ongoing. This specific propagation conditions allowed us to compute attenuation simply considering the C_{eff_ratio} within the stratospheric duct. Results allow to track the multi-year variation of explosive intensity, but fail investigating seasonal variations due to larger uncertainties around the equinoxes, when wind reverse and models are less reliable (Assink et al., 2014).

Results of this study showed however that for Yasur volcano a quantitative assessment of the variation of explosive intensity can be achieved by considering the maximum range corrected pressure and the persistency of the signal (IP), that suggest a clear increase of explosive activity starting from 2016; it is tracked also with satellite-borne thermal infrared imagery. Such an information, which is not that evident from local observations and assessments, might reflect a slight variation in the gas/magma input rate that is driving the sustained persistent explosive activity of the volcano and might provide a useful constraint for additional local investigations and hazard assessments.

Despite being site specific, results presented in this confirm that long range infrasound can provide quantitative information on the activity level at a low energy, persistent, explosive volcano, such as Yasur, at time scales varying from minutes (time of occurrence and amplitude of single explosions) to decades (mean energy release). Corroborating more and more studies on the operational use of long-range infrasound for volcano monitoring (e.g. Matoza et al., 2011b; Fee et al., 2013; Coombs et al., 2018; Marchetti et al., 2019; Le Pichon et al., 2021; Ortiz et al., 2021, among the others), presented results remind how long-range infrasound might be consider to integrate satellite observations for active volcanoes around the world in areas that are missing local monitoring systems, and could be used routinely for integrated volcano monitoring solutions at regional scales. The International Civil Aviation Organization (ICAO) expressed an interest in the potential of global and regional infrasound networks to provide eruption notifications to the aviation community through the existing international Volcanic Ash Advisory Centre (VAAC) framework (http://www.ssd.noaa.gov/VAAC/vaac.html) (Garcés et al., 2008).

Credit author statement

Rebecca Sveva Morelli: Data curation, Resources, Writing - original draft, Visualization, Validation;
Duccio Gheri: Reviewing, Editing;
Paola Campus: Data Curation, Reviewing, Validation;
Diego Coppola: Data Curation, Reviewing, Validation;
Emanuele Marchetti: Conceptualization, Data Curation, Supervision, Validation, Methodology, Reviewing, Writing - rewiw & editing, Editing.

Disclaimer

The views expressed herein are those of the author(s) and do not necessarily reflect the views of the CTBTO Preparatory Commission.

Declaration of Competing Interest

The authors declare that they have no known competing financial interests or personal relationships that could have appeared to influence the work reported in this paper.

The authors declare the following financial interests/personal relationships which may be considered as potential competing interests:

Rebecca Sveva Morelli reports writing assistance was provided by Preparatory Commission for the Comprehensive Nuclear-Test-Ban Treaty Organization.

Data availability

Data will be made available on request.

Acknowledgements

The authors are grateful to the Comprehensive Nuclear-Test-Ban Treaty Organization for guaranteeing access to the high-quality infrasound data. This study was facilitated by previous research performed within the framework of the 'Atmospheric dynamics Research Infra-Structure in Europe' (ARISE) project, funded by the European Commission FP7 and Horizon 2020 programs (Grant agreements 284387 and 653980).

References

Acharya, P., Sreekesh, S., 2013. Seasonal variability in aerosol optical depth over India: a spatio-temporal analysis using the MODIS aerosol product. Int. J. Remote Sens. 34 (13), 4832–4849. https://doi.org/10.1080/01431161.2013.782114.

Alcoverro, B., Le Pichon, A., 2005. Design and optimization of a noise reduction system for infrasonic measurements using elements with low acoustic impedance. J. Acoust. Soc. Am. 117 (4), 1717–1727. https://doi.org/10.1121/1.1804966.

Antier, K., Le Pichon, A., Vergniolle, S., Zielinski, C., Lardy, M., 2007. Multiyear validation of the NRL-G2S wind fields using infrasound from Yasur. J. Geophys. Res.-Atmos. 112 (D23) https://doi.org/10.1029/2007JD008462.

Assink, J.D., Waxler, R., Drob, D., 2012. On the sensitivity of infrasonic traveltimes in the equatorial region to the atmospheric tides. J. Geophys. Res.-Atmos. 117 (D1) https://doi.org/10.1029/2011JD016107.

Assink, J.D., Waxler, R., Frazier, W.G., Lonzaga, J., 2013. The estimation of upper atmospheric wind model updates from infrasound data. J. Geophys. Res.-Atmos. 118 (19), 10–707. https://doi.org/10.1002/jgrd.50833.

Arnoult, K.M., Olson, J.V., Szuberla, C.A., McNutt, S.R., Garcés, M.A., Fee, D., Hedlin, M. A., 2010. Infrasound observations of the 2008 explosive eruptions of Okmok and Kasatochi volcanoes, Alaska. J. Geophys. Res. Atmos. 115 (D2) https://doi.org/10.1029/2010JD013987.

Assink, J.D., Le Pichon, A., Blanc, E., Kallel, M., Khemiri, L., 2014. Evaluation of wind and temperature profiles from ECMWF analysis on two hemispheres using volcanic infrasound. J. Geophys. Res. Atmos. 119 https://doi.org/10.1002/2014JD021632.

Bani, P., Lardy, M., 2007. Sulphur dioxide emission rates from Yasur volcano, Vanuatu archipelago. Geophys. Res. Lett. Solid Earth. https://doi.org/10.1029/2007GL030411.

Battaglia, J., Métaxian, J.P., Garaebiti, E., 2016. Short term precursors of Strombolian explosions at Yasur volcano (Vanuatu). Geophys. Res. Lett. 43, 1960–1965. https://doi.org/10.1002/2016GL067823.

Berger, M., Moreno, J., Johannessen, J.A., Levelt, P.F., Hanssen, R.F., 2012. ESA's sentinel missions in support of Earth system science. Remote Sens. Environ. https://doi.org/10.1016/j.rse.2011.07.023.

Brown, S.K., Jenkins, S.F., Sparks, R.S.J., Odbert, H., Auker, M.R., 2017. Volcanic fatalities database: analysis of volcanic threat with distance and victim classification. J. Appl. Volcanol. 6, 15. https://doi.org/10.1186/s13617-017-0067-4.

Campus, P., Christie, D.R., 2010. Worldwide observations of infrasonic waves. In: Pichon, A.L., Blanc, E., Hauchecorne, A. (Eds.), Infrasound Monitoring for Atmospheric Studies. Springer, Netherlands, pp. 185–234. https://doi.org/10.1007/978-1-4020-9508-5_2 chap. 2.

Cansi, Y., 1995. An automatic seismic event processing for detection and location: the PMCC method. Geophys. Res. Lett. 22 (9), 1021–1024. https://doi.org/10.1029/95GL00468.

Carn, S., Fioletov, V., McLinden, C.L., Krotkov, N.A., 2017. A decade of global volcanic SO2 emissions measured from space. Sci. Rep. 7, 44095. https://doi.org/10.1038/srep44095.

Christie, D.R., Campus, P., 2010. The IMS infrasound network: Design and establishment of infrasound stations. In: Pichon, A.L., Blanc, E., Hauchecorne, A. (Eds.), Infrasound Monitoring for Atmospheric Studies. Springer, Netherlands, pp. 29–75. https://doi.org/10.1007/978-1-4020-9508-5_2 chap. 2.

Coombs, M.L., Wech, A.G., Haney, M.M., Lyons, J.J., Schneider, D.J., Schwaiger, H.F., Wallace, K.L., Fee, D., Freymueller, J.T., Schaefer, J.R., Tepp, G., 2018. Short-term forecasting and detection of explosions during the 2016–2017 eruption of Bogoslof volcano, *Alaska*. Fronti. Earth Sci. 6, 122. https://doi.org/10.3389/feart.2018.00122.

Coppola, D., Piscopo, P., Laiolo, M., Cigolini, C., Delle Donne, D., Ripepe, M., 2012. Radiative heat power at Stromboli volcano during 2000-2011: twelve years of MODIS observations. J. Volcnol. Geoth. Res. 215-216, 48–60. https://doi.org/10.1016/j.volgeores.2011.12.001.

Coppola, D., Laiolo, M., Cigolini, C., Delle Donne, D., Ripepe, M., 2016a. Enhanced volcanic hotspot detection using MODIS IR data: Results from the MIROVA system. In: Harris, A.J.L., et al. (Eds.), Detecting, Mod− elling and Responding to Effusive Eruptions: Geological Society of London Special Publication, 426, pp. 181–205. https://doi.org/10.1144/SP426.5.

Coppola, D., Laiolo, M., Cigolini, C., 2016b. Fifteen years of thermal activity at Vanuatu's volcanoes (2000-2015) revealed by MIROVA. J. Volcanol. Geotherm. Res. 322, 6–10. https://doi.org/10.1016/j.jvolgeores.2015.11.005.

Dabrowa, A.L., Green, D.N., Rust, A.C., Phillips, J.C., 2011. A global study of volcanic infrasound characteristics and the potential for long-range monitoring, Earth Planet. Sci. Lett. 310, 369–379. https://doi.org/10.1016/j.epsl.2011.08.027.

Dabrowa, A.L., Green, D.N., Johnson, J.B., Phillips, J.C., Rust, A.C., 2014. Comparing near-regional and local measurements of infrasound from Mount Erebus, Antarctica: implications for monitoring. J. Volcanol. Geotherm. Res. 288, 46–61. https://doi.org/10.1016/j.jvolgeores.2014.10.001.

De Negri, R.S., Rose, K.M., Matoza, R.S., Hupe, P., Ceranna, L., 2022. Long-range multi-year infrasonic detection of eruptive activity at Mount Michael Volcano, South Sandwich Islands. Geophys. Res. Lett. 49 (7) https://doi.org/10.1029/2021GL096061 e2021GL096061.

Drob, D.P., Picone, J.M., Garcés, M., 2003. Global morphology of infrasound propagation. J. Geoph. R.: Atmos. 108, D21. https://doi.org/10.1029/2002JD003307.

Dzurisin, D., 2003. A comprehensive approach to monitoring volcano deformation as a window on the eruption cycle. Rev. Geophys. https://doi.org/10.1029/2001RG000107.

Fee, D., Garces, M., Orr, T., Poland, M., 2011. Infrasound from the 2007 fissure eruptions of Kīlauea Volcano, Hawai'i. Geophys. Res. Lett. 38 (6) https://doi.org/10.1029/2010GL046422.

Fee, D., Garces, M., Steffke, A., 2010. Infrasound from Tungurahua volcano 2006–2008: Strombolian to Plinian eruptive activity. J. Volcanol. Geotherm. Res. 193 (1–2), 67–81. https://doi.org/10.1016/j.jvolgeores.2010.03.006.

Fee, D., Matoza, R.S., 2013. An overview of volcano infrasound: from Hawaiian to Plinian, local to global. J. Volcanol. Geotherm. Res. 249, 123–139. https://doi.org/10.1016/j.jvolgeores.2012.09.002.

Fee, D., McNutt, S.R., Lopez, T.M., Arnoult, K.M., Szuberla, C.A., Olson, J.V., 2013. Combining local and remote infrasound recordings from the 2009 Redoubt Volcano eruption. J. Volcanol. Geotherm. Res. 259, 100–114. https://doi.org/10.1016/j.jvolgeores.2011.09.012.

Garcés, M., Fee, D., Steffke, A., McCormack, D., Servranckx, R., Bass, H., Hetzer, C., Hedlin, M., Matoza, R., Yepes, H., Ramon, P., 2008. Capturing the acoustic fingerprint of stratospheric ash injection. EOS Trans. Am. Geophys. Union 89 (40), 377–378. https://doi.org/10.1029/2008EO400001.

Garces, M., Hetzer, C., 2002. Evaluation of infrasonic detection algorithms. This volume.

Global Volcanism Program, 2022. Smithsonian Institution. https://volcano.si.edu/.

Harris, A., 2013. Thermal Remote Sensing of Active Volcanoes: A user's Manual. Cambridge University Press. ISBN 978-0-521-85945-5.

Iezzi, A.M., Matoza, R.S., Bishop, J.W., Bhetanabhotla, S., Fee, D., 2022. Narrow-band least-squares infrasound array processing. Seismol. Soc. Am. 93 (5), 2818–2833. https://doi.org/10.1785/0220220042.

Jolly, A.D., Matoza, R.S., Fee, D., Kennedy, B.M., Iezzi, A.M., Fitzgerald, R.H., Austin, A. C., Johnson, R., 2017. Capturing the acoustic radiation pattern of strombolian eruptions using infrasound sensors aboard a tethered aerostat, Yasur volcano, *Vanuatu*. Geophys. Res. Lett. 44 (19), 9672–9680. https://doi.org/10.1002/2017GL074971.

Khan, M.M., Alparone, L., Chanussot, J., 2009. Pansharpening quality assessment using the modulation transfer functions of instruments. IEEE Trans. Geosci. Remote Sens. 47 (11), 3880–3891. https://doi.org/10.1109/TGRS.2009.2029094.

Kim, Y., Moorcroft, P.R., Aleinov, I., Puma, M.J., Kiang, N.Y., 2015. *Variability of phenology and fluxes of water and carbon with observed and simulated soil moisture in the Ent Terrestrial Biosphere Model* (Ent TBM version 1.0.1.0.0). Geosci. Model Dev. https://doi.org/10.5194/gmd-8-3837-2015.

Le Pichon, A., Blanc, E., Drob, D., 2005a. Probing high-altitude winds using infrasound. J. Geophys. Res.-Atmos. 110 (D20) https://doi.org/10.1029/2005JD006020.

Le Pichon, A., Blanc, E., Drob, D., Lambotte, S., Dessa, J.X., Lardy, M., Bani, P., Vergniolle, S., 2005b. Infrasound monitoring of volcanoes to probe high-altitude winds. J. Geophys. Res. 110 https://doi.org/10.1029/2004JD005587. D13106.

Le Pichon, A., Matoza, R., Brachet, N., Cansi, Y., 2010. Recent enhancements of the PMCC infrasound signal detector. Inframatics 26, 5–8.

Le Pichon, A., Ceranna, L., Vergoz, J., 2012. Incorporating numerical modeling into estimates of the detection capability of the IMS infrasound network. J. Geophys. Res. 117 https://doi.org/10.1029/2011JD016670. D05121.

Le Pichon, A., Pilger, C., Ceranna, L., Marchetti, E., Lacanna, G., Souty, V., Vergoz, J., Listowski, C., Hernandez, B., Mazet-Roux, G., Dupont, A., Hereil, P., 2021. Using dense seismo-acoustic network to provide timely warning of the 2019 paroxysmal Stromboli eruptions. Sci. Rep. 11, 14464. https://doi.org/10.1038/s41598-021-93942-x.

Marchetti, E., Ripepe, M., Delle Donne, D., Genco, R., Finizola, A., Garaebiti, E., 2013. Blast waves from violent explosive activity at Yasur volcano, Vanuatu. Geophys. Res. Lett. 40, 5838–5843. https://doi.org/10.1002/2013GL057900.

Marchetti, E., Ripepe, M., Campus, P., Le Pichon, A., Vergoz, J., Lacanna, G., Mialle, P., Héreil, P., Husson, P., 2019. Long range infrasound monitoring of Etna volcano. Nat. Sci. Rep. 9, 18015. https://doi.org/10.1038/s41598-019-54468-5.

Matoza, R.S., Le Pichon, A., Vergoz, J., Herry, P., Lalande, J.M., Lee, H., Che, I., Rybin, A., 2011a. Infrasonic observations of the June 2009 Sarychev Peak eruption, Kuril Islands: Implications for infrasonic monitoring of remote explosive volcanism. J. Volcanol. Geotherm. Res. 200, 35–48. https://doi.org/10.1016/j.jvolgeores.2010.11.022.

Matoza, R.S., Vergoz, J., Le Pichon, A., Ceranna, L., Green, D.N., Evers, L.G., Ripepe, M., Campus, P., Liszka, L., Kvaerna, T., Kjartansson, E., Höskuldsson, Á., 2011b. Long-range acoustic observations of the Eyjafjallajökull eruption, Iceland, April-May 2010. Geophys. Res. Lett. 38 (6) https://doi.org/10.1029/2011GL047019.

Matoza, R.S., Green, D.N., Le Pichon, A., Shearer, P.M., Fee, D., Mialle, P., Ceranna, L., 2017. Automated detection and cataloging of global explosive volcanism using the international monitoring system infrasound network. JGR Solid Earth. https://doi.org/10.1002/2016JB013356.

Matoza, R.S., Fee, D., Green, D., Mialle, P., 2019. Volcano infrasound and the international monitoring system. In: Le Pichon, A., Blanc, E., Hauchecorne, A. (Eds.), Infrasound Monitoring for Atmospheric Studies. Springer, Cham. https://doi.org/10.1007/978-3-319-75140-5_33.

Meier, K., Hort, M., Wassermann, J., Garaebiti, E., 2016. Strombolian surface activity regimes at Yasur volcano, Vanuatu, as observed by Doppler radar, infrared camera and infrasound. J. Volcanol. Geotherm. Res. 322, 184–195. https://doi.org/10.1016/j.jvolgeores.2015.07.038.

Ortiz, H.D., Matoza, R.S., Garapaty, C., Rose, K., Ramón, P., Ruiz, M.C., 2021. Multi-year regional infrasound detection of Tungurahua, El Reventador, and Sangay volcanoes in Ecuador from 2006 to 2013. In: Proceedings of Meetings on Acoustics LRSP, vol. 41. Acoustical Society of America. https://doi.org/10.1121/2.0001362. No. 1, p. 022003.

Pallister, J., McNutt, S.R., 2015. Chapter 66 - Synthesis of Volcano Monitoring. In: The Encyclopedia of Volcanoes, , Second edition2015. Academic Press, pp. 1151–1171. ISBN 9780123859389. https://doi.org/10.1016/B978-0-12-385938-9.00066-3.

Peltier, A., Finizola, A., Douillet, G.A., Brothelande, E., Garaebiti, E., 2012. Structure of an active volcano associated with a resurgent block inferred from thermal mapping: The Yasur–Yenkahe volcanic complex (Vanuatu). J. Volcanol. Geotherm. Res. 243–244, 59–68. https://doi.org/10.1016/j.jvolgeores.2012.06.022, 15 October 2012.

Perttu, A., Taisne, B., De Angelis, S., Assink, J.D., Tailpied, D., Williams, R.A., 2020. Estimates of plume height from infrasound for regional volcano monitoring. J. Volcanol. Geotherm. Res. 402, 106997 https://doi.org/10.1016/j.jvolgeores.2020.106997.

Phillipson, G., Sobradelo, R., Gottsmann, J., 2013. Global volcanic unrest in the 21st century: an analysis of the first decade. J. Volcanol. Geotherm. Res. https://doi.org/10.1016/j.jvolgeores.2013.08.004.

Pilger, C., Ceranna, L., Ross, J.O., Vergoz, J., Le Pichon, A., Brachet, N., Blanc, E., Kero, J., Liszka, L., Gibbons, S., Kvaerna, T., Näsholm, S.P., Marchetti, E., Ripepe, M., Smets, P., Evers, L., Ghica, D., Ionescu, C., Sindelarova, T., Ben Horin, Y., Mialle, P., 2018. The European infrasound bulletin. Pure Appl. Geophys. 175 (10), 3619–3638. https://doi.org/10.1007/s00024-018-1900-3.

Pinel, V., Poland, M.P., Hooper, A., 2014. Volcanology: lessons learned from synthetic aperture radar imagery. J. Volcanol. Geotherm. Res. https://doi.org/10.1016/j.jvolgeores.2014.10.010.

Ramsey, M., Realmuto, V.J., Hulley, G.C., Hook, S.J., 2012. HyspIRI thermal infrared (TIR) band study report. JPL Publ. 12 (16), 1–49. https://hyspiri.jpl.nasa.gov/downloads/reports_whitepapers/HyspIRI_TIR_Band_Report_gchv1_VJRv1_pmbv1_MSRv2_1.pdf.

Ripepe, M., Marchetti, E., Delle Donne, D., Genco, R., Innocenti, L., Lacanna, G., Valade, S., 2018. Infrasonic early warning system for explosive eruptions. J. Geophys. Res.: Solid Earth 123 (11), 9570–9585. https://doi.org/10.1029/2018JB015561.

Rose, K.M., Matoza, R.S., 2021. Remote hydroacoustic-infrasonic detection and characterization of Anak Krakatau eruptive activity leading to, during, and following the December 2018 flank collapse and tsunami. Bull. Volcanol. 83 (8), 1–17. https://doi.org/10.1007/s00445-021-01468-x.

Schwaiger, H.F., Iezzi, A.M., Fee, D., 2019. AVO-G2S: *a modified, open-source ground-to-space atmospheric specification for infrasound modeling.* Comput. Geosci. 125, 90–97. https://doi.org/10.1016/j.cageo.2018.12.013.

Schwaiger, H.F., Lyons, J.J., Iezzi, A.M., Fee, D., Haney, M.M., 2020. Evolving infrasound detections from Bogoslof volcano, Alaska: insights from atmospheric propagation modeling. Bull. Volcanol. 82 (3), 1–14. https://doi.org/10.1007/s00445-020-1360-3.

Sparks, R.S.J., Aspinall, W.P., Crosweller, H.S., Hincks, T.K., 2013. Risk and uncertainty assessment of volcanic hazards. In: Rougier, J., Sparks, R.S.J., Hill, L.J. (Eds.), Risk and Uncertainty Assessment for Natural Hazards. Cambridge University Press, pp. 364–397. https://doi.org/10.1017/CBO9781139047562.012.

Spina, L., Taddeucci, J., Cannata, A., Gresta, S., Lodato, L., Privitera, E., Scarlato, P., Gaeta, M., Gaudin, D., Palladino, D.M., 2015. Explosive volcanic activity at Mt. Yasur: a characterization of the acoustic events (9–12th July 2011). J. Volcanol. Geotherm. Res. 302 (2015), 24–32. https://doi.org/10.1016/j.jvolgeores.2015.07.027.

Tailpied, D., Le Pichon, A., Marchetti, E., Assink, J., Vergniolle, S., 2016. Assessing and optimizing the performance of infrasound networks to monitor volcanic eruptions. Geophys. J. Int. Oxf. Univ. Press (OUP) 208 (1), 437–448. https://doi.org/10.1093/gji/ggw400.

Tailpied, D., Le Pichon, A., Taisne, B., 2022. Assessing uncertainties in infrasound network performance modelling: application to the Euro-Mediterranean and Southeast Asian region. Geophys. J. Int. 228 (2), 1324–1345. https://doi.org/10.1093/gji/ggab399.

Taisne, B., Perttu, A., Tailpied, D., Caudron, C., Simonini, L., 2019. Atmospheric controls on ground- and space-based remote detection of volcanic ash injection into the atmosphere, and link to early warning systems for aviation hazard mitigation. In: Le Pichon, A., Blanc, E., Hauchecorne, A. (Eds.), Infrasound Monitoring for Atmospheric Studies. Springer, Cham. https://doi.org/10.1007/978-3-319-75140-5_34.

Theys, N., Hedelt, P., De Smedt, I., Lerot, C., Yu, H., Vlietinck, J., Pedergnana, M., Arellano, S., Galle, B., Fernandez, D., Carlito, C.J.M., Barrington, C., Taisne, B., Delgado-Granados, H., Loyola, D., Van Roozendael, M., 2019. Global monitoring of volcanic SO2 degassing with unprecedented resolution from TROPOMI onboard Sentinel-5 Precursor. Sci. Rep. 9, 2643. https://doi.org/10.1038/s41598-019-39279-y.

Ulivieri, G., Marchetti, E., Ripepe, M., Chiambretti, I., Derosa, G., Segor, V., 2011. Monitoring snow avalanches in Northwestern Italian Alps using an infrasound array. Cold Reg. Sci. Technol. 69, 177–183. https://doi.org/10.1016/j.coldregions.2011.09.006.

Ulivieri, G., Ripepe, M., Marchetti, E., 2013. Infrasound reveals to oscillatory discharge regime during lava fountaining: implication for early warining. Geoph. Res. Lett. 40, 1–6. https://doi.org/10.1002/grl.50592.

Valade, S., Ley, A., Massimetti, F., D'Hondt, O., Laiolo, M., Coppola, D., Loibl, D., Hellwich, O., Walter, T.R., 2019. Towards global volcano monitoring usingmultisensor sentinel missions and artificial intelligence: the MOUNTS monitoring system. Remote Sens. 11, 1528. https://doi.org/10.3390/rs11131528.

Wright, R., Flynn, L., Garbeil, H., Harris, A., Pilger, E., 2002. Automated volcanic eruption detection using MODIS. Remote Sens. Environ. 82 (1), 135–155. https://doi.org/10.1016/S0034-4257(02)00030-5.

Zhang, J., Reid, J.S., 2009. An analysis of clear sky and contextual biases using an operational over ocean MODIS aerosol product. Geophys. Res. Lett. 36 (15) https://doi.org/10.1029/2009GL038723.